YALE JOURNAL OF BIOLOGY AND MEDICINE 96 (2023), pp.3-12.

ORIGINAL CONTRIBUTION

YALE JOURNAL OF BIOLOGY AND MEDICINE
YJBM
CELEBRATING 95 YEARS 1928–2023

Design and Characterization of Nanoflowers-based Biosensor for Estimation of Bilirubin in Jaundice

Kanchi Acharya, Bala Prabhakar, and Pravin Shende*

Shobhaben Pratapbhai Patel School of Pharmacy & Technology Management, Mumbai, India

Nanoflowers (NFs) are flower-shaped nanoparticulate systems with a higher surface-to-volume ratio and good surface adsorption. Jaundice indicates yellow discoloration of skin, sclera, and mucus membrane and is a clinical indication of bilirubin accumulation in the blood which occurs as a consequence of the incapability of the liver to excrete bilirubin in the biliary tree or conjugate bilirubin and higher production of bilirubin in the body. Several methods have been developed so far for bilirubin estimation in jaundice like the spectrophotometric method, chemiluminescence method, etc., but biosensing methods provide advantages over traditional methods concerning the surface area, adsorption, particle size, and functional characteristics. The primary objective of the present research project was to formulate and examine the adsorbent nanoflowers-based biosensor for accurate, precise, and sensitive detection of bilirubin in jaundice. The particle size of adsorbent nanoflowers was found to be in the range of 300-600nm with the surface charge (zeta potential) in the range of -1.12 to -15.42 mV. Transmission electron microscopy and scanning electron microscopy images confirmed the flower-like morphological structure of adsorbent NFs. The adsorption efficiency of NFs for bilirubin adsorption was maximum at 94.13%. Comparative studies of bilirubin estimation in the pathological sample with adsorbent NFs and diagnostic kit displayed bilirubin concentration to be 1.0 mg/dL in adsorbent nanoflowers and 1.1 mg/dL with diagnostic kit indicating effective detection of bilirubin with adsorbent NFs. The nanoflower-based biosensor acts as a smart approach to elevate adsorption efficiency on the surface of nanoflower due to a higher surface-to-volume (SV) ratio.

INTRODUCTION

Nanoflowers (NFs) are flower-shaped nanoparticulate systems with various applications in bio-sensing, drug delivery, catalysis, optoelectronic device, etc. [1]. Different processes are used for the synthesis of NFs, like immobilization methods, crosslinking methods, conjugation methods, and self-gathering methods [2,3]. NFs are made up of different layers of petals, which render the increased surface area comparatively smaller in struc-

*To whom all correspondence should be addressed: Dr. Pravin Shende, Shobhaben Pratapbhai Patel School of Pharmacy and Technology Management, Mumbai, India; Email: shendepravin94@gmail.com.

Abbreviations: NF, Nanoflowers; SV, surface-to-volume; CN syndrome, Crigler-Najjar syndrome; STPP, sodium tripolyphosphate; FE-SEM, field emission scanning electron microscopy; TEM, transmission electron microscopy; XRPD, X-ray powder diffraction spectroscopy; DSC, differential scanning calorimetry; NMR, nuclear magnetic resonance spectroscopy; FTIR, Fourier-Transform infrared spectroscopy; TGA, thermal gravimetric analysis; DTA, differential thermal analysis; PS, particle size; SC, surface charge; PDI, polydispersity index.

Keywords: Adsorption capacity, bilirubin, biosensor, adsorbent nanoflowers, inotropic gelation technique

Author Contributions: KA: Visualization, writing (original draft); BP: Visualization, writing (review and editing); PS: Conceptualization, writing (review and editing), supervision.

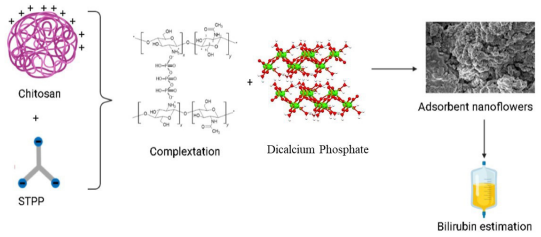

Graphical Abstract

ture to facilitate their application in various areas like biosensing, catalysis, purification, and drug delivery [1]. The present applications of NFs include gene carriers, photosensitizers, photothermal treatment, detection of various diseases like neurodegenerative conditions, diabetes, and food infection. Also, NFs extend new aspects in many fields such as purification of enzymes, removal of dyes and heavy metals from water. Due to a higher surface-to-volume (SV) ratio with greater surface adsorption, NFs showed faster reaction kinetics. On the basis of the particle size and morphological structure, NFs show increased stability and better adsorption efficiency and are the preferred choice of nanoparticulate systems attributable to their relatively simple method of synthesis and cost-effective and non-toxic properties [3-6].

Jaundice indicates yellow discoloration of skin, sclera, and mucus membranes and is a clinical indication of bilirubin accumulation in the blood, which occurs as a consequence of the incapability of the liver to excrete bilirubin in the biliary tree or conjugate bilirubin and higher production of bilirubin in the body [6]. Normal serum bilirubin levels are <17 µmol/L and in the case of jaundice, the serum bilirubin levels increase to >34 µmol/L [7]. Serum bilirubin levels are used as a biomarker to help diagnose several liver illnesses, such as Gilbert syndrome, CN syndrome (Crigler-Najjar syndrome), Robert syndrome, and in severe cases, bilirubin encephalopathy. Bilirubin is a catabolically produced, yellow tetrapyrrole compound produced by the degradation of red blood cells (RBCs). The end product of RBCs in the blood vessel is bilirubin, and bilirubin is accumulated with albumin conjugates with glucuronic acid in the liver. This concentrated bilirubin along with bile constituents in the gall bladder breaks down into bilirubin and acid, which leads to blockages of passages due to the absorption of bilirubin in blood serum, elevating the levels of bilirubin in the blood leading to hyperbilirubinemia [6,8,9]. Bilirubin detection methods employed earlier were mainly dependent on the oxidation product of bilirubin, biliverdin, which showed interference of pigments like carotene, hemoglobins, and xanthophylls in bilirubin assessment limiting the efficacy and sensitivity of the technique [10,11]. Different methods used for bilirubin estimation in biological samples are the direct spectroscopic method, diazo reaction method [12], fluorometry, high-pressure liquid chromatography, and enzymatic assay [13,14]. This set of methods employed for bilirubin estimation in jaundice requires expensive instrumentations, extensive time, and highly skilled labor. Adsorption is an effective and reliable technique for the estimation of biological compounds from serum. To overcome the limitations of conventional methods–(diazo method, vanadate oxidase method, capillary electrophoresis, and fluorometry) like sensitivity concerning change in environment, expensive instrumentation, results influenced by the change in moisture and temperature, and requirement of costly chemicals–nanoparticulate systems are developed [10]. Chitosan (CS) is a biodegradable, biocompatible, and naturally occurring polymer and possesses three functional groups [15]. Nanoflowers-based biosensors for bilirubin estimation in jaundice were prepared using the inotropic gelation technique. The effective complexation between polymer and cross-linker; CS and sodium tripolyphosphate (STPP) displayed the formation of complexation leading to the formation of nanoflowers. Due to higher surface area and SV ratio, biosensor-based adsorbent nanoflowers are novel nano-formulation systems, used for increased adsorption efficiency (%) and adsorption capacity. The focus of this research was to suggest and examine the adsorption behavior of NFs for bilirubin quantification in jaundice. Dissolution of polymer (CS) in an acidic medium leads to the formation of cationic group NH_3^+. At pH 9.1, hydroxide and phosphoric ions existing in STPP solution, reacts with NH_3^+ in CS, where hydroxide ions in STPP solution are accountable for deprotonation of CS resulting in crosslinking of polymer and cross-linker.

MATERIALS AND METHODS

Materials

Bilirubin ($C_{33}H_{36}N_4O_6$), and Dicalcium Phosphate (CaHPO4) were obtained from Loba Chemie, Mumbai, India. STPP was procured from Research Lab, Mumbai, India. CS was purchased from SISCO Research Laboratories Pvt. Ltd. Mumbai, India. Erba Bilirubin (Total) biochemistry reagent (4*60 ml) was procured from Erba Mannheim. All other compounds and reagents that were utilized were of analytical grade.

Methods

Preparation of Adsorbent Nanoflowers: The ionotropic gelation technique was used for the preparation of adsorbent nanoflowers using CS, STPP with DCP in the ratios of 1:3.5:1 (% w/w) as illustrated in Table 1. CS

Table 1. Composition of Adsorbent Nanoflowers

Composition	Formulation					
	KA1	KA2	KA3	KA4	KA5	KA6
Chitosan (CS)	1 %	1 %	1 %	1 %	1 %	1 %
Sodium tripolyphosphate (STPP)	1 %	1.5 %	2 %	2.5 %	3 %	3.5 %
Dicalcium Phosphate (DCP)	1 %	1 %	1 %	1 %	1 %	1 %

solution (1%) was prepared under continuous stirring. To 1% CS solution, 3.5% of aqueous STPP was added drop by drop under continuous stirring for 30 min. Then, 1% DCP solution was added to the above-prepared solution and stirred for 30 min. The resultant solution was probe sonicated for 30 min, then centrifuged at 8000 rpm for 10 min at 25°C and the product obtained was allowed to dry at room temperature. The prepared NFs were abbreviated as KA6. The composition of adsorbent nanoflowers are stated in Table 1.

Characterization of Adsorbent Nanoflowers: The particle size (PS), surface charge (SC), and polydispersity index (PDI) of adsorbent nanoflowers (KA1-KA6) were studied using Malvern zeta seizer (MAL 1118512 UK) with double distilled water as the dispersion medium at ambient temperature by light scattering technique. Based on results from particle size, surface charge, % adsorption efficiency (AE), and adsorption capacity; formulation KA6 was further characterized for; field emission scanning electron microscopy (FE-SEM), transmission electron microscopy (TEM), Attenuated total reflectance-Fourier transform infrared spectroscopy (ATR-FTIR), differential scanning calorimetry (DSC), nuclear magnetic resonance spectroscopy (NMR), thermal gravimetric analysis (TGA), and differential thermal analysis (DTA). FE-SEM and TEM of formulation KA6 were assessed for the morphology of adsorbent nanoflowers. The chemical characteristics include functional groups and chemical interactions between different excipients of blank adsorbent nanoflower KA6: bilirubin adsorbed nanoflower formulation KA6, CS, STPP, and DCP were examined with ATR-FTIR spectroscopy (Perkin Elmer, USA) at the wavelength of 400-4000 cm^{-1}. Thermal analysis of KA6 was observed using DSC (Mettler Toledo, Switzerland). For the DSC studies, KA6 was sealed in aluminum pans with a temperature range of 30-300 °C, at a flow rate of 10 °C/min with N_2 purge. Formulation KA6 was also characterized for TGA and DTA (Shimadzu, Japan).

Adsorption Studies of Nanoflowers

The Influence of Bilirubin Levels on Adsorption: The impact of bilirubin concentration on % AE and adsorption capacity was investigated with a 10 mL bilirubin sample solution using phosphate buffer (PB) pH 7.4 as a solvent with various concentrations (100, 120, 140, 160, and 180 ppm) of bilirubin. To the prepared bilirubin sample solutions, 5 mg adsorbent nanoflowers were added and the resulting solution was agitated in an orbital shaker for 2-3 h, following which the concentration of bilirubin in supernatants is examined under a UV-visible spectrophotometer (Shimadzu, Japan) at 440 nm. The % AE along with adsorption capacity of nanoflowers on different concentrations of bilirubin was monitored from the results.

Using the formula, the adsorption efficiency of NFs was computed:

$$Adsorption\ efficiency\ (\%) = \frac{(Co - Ct)}{Co} \text{x} 100$$

Where, *Co*: concentration of bilirubin (mgL^{-1}), *Ct*: equilibrium bilirubin concentration in solution (mgL^{-1})

The adsorption capacity of NFs was determined by the following formula:

$$Adsorption\ Capacity\ (qe) = \frac{(Co - Ct)\,V}{m}$$

Where, *qe*: Adsorption capacity, *Co*: concentration of bilirubin (mgL^{-1}), m: adsorbent nanoflower mass (g), *Ct*: equilibrium bilirubin concentration in solution (mgL^{-1}), and *V*: volume of solution (ml).

Impact of The Number of Adsorbent Nanoflowers: The impact of concentration of adsorbent on % AE and adsorption capacity was investigated with 10 mL bilirubin sample solution using PB pH 7.4 as a solvent with various amounts (6, 12, 18, 24, and 30 mg) of NFs. The resulting solution was agitated in an orbital shaker for 2-3 h, following which the concentration of bilirubin in supernatants was studied using a UV-visible spectrophotometer (Shimadzu, Japan) at 440nm. The data were used to calculate the % AE and capacity of nanoflowers with various amounts of adsorbents.

Desorption Studies: A desorption study for adsorbent NFs was conducted to examine the re-utilization of NFs for bilirubin adsorption. The bilirubin adsorbed nanoflowers were suspended into PB pH 7.4 and bioactive NFs were separated from the solution using centrifugation and washed with PB pH 7.4. For subsequent bilirubin estimation, the bioactive nanoflowers were filtered

Table 2. PS, SC, and PDI

Formulation	PS (nm ± S.D.)	SC (mV± S.D.)	PDI
KA1	647.26±6.12	-15.26±0.38	0.56±0.21
KA2	531.40±4.31	-15.20±0.37	0.55±0.03
KA3	441.23±5.54	-15.20±0.21	0.46±0.37
KA4	431.96±5.53	-15.90±0.57	0.42±0.02
KA5	415.31±5.96	-15.10±0.03	0.49±0.51
KA6	332.96±6.21	-14.10±0.16	0.42±0.27

and re-dispersed in a 10 mL fresh sample solution.

Artificial Urine Sample Study of Nanoflowers: Ten-milliliter artificial urine samples with varying concentrations of bilirubin from 1 mg/dL to 5 mg/dL were prepared. Five-milligram NFs were added to the above prepared artificial urine samples and the resulting solutions were kept in an orbital shaker for 2-3 h following which the concentration of bilirubin in supernatants is examined with a UV-visible spectrophotometer (Shimadzu, Japan) at 440nm. The % AE and adsorption capacity of NFs in artificial urine were estimated from the results.

Pathological Sample Study of Nanoflowers: For the real-time studies of bilirubin estimation in jaundice, five patients with jaundice were examined in Cooper Hospital (Mumbai, India). Five-milligram NFs were added to the urine samples of patients and the resulting solutions were kept in an orbital shaker for 2-3 h following which the concentration of bilirubin in supernatants was examined under a UV-visible spectrophotometer (Shimadzu, Japan) at 440nm. Percent AE and adsorption capacity of NFs in the pathological urine sample were estimated from the results. Negative urine samples were considered as control group. For bilirubin estimation by diagnostic kit, 10 mL working reagent using total bilirubin reagent and sodium nitrile reagent was prepared. To the prepared working reagent, test solution (pathology urine samples) were added and the resulting solution was examined for total bilirubin concentration by the diazo method using the Erba biochemistry analyzer. The same procedure for pathology sample studies using nanoflowers was followed and the comparative study for bilirubin estimation by adsorbent nanoflowers and the diagnostic kit was studied. The adsorption-based experiments of adsorbent nanoflowers were performed in triplicate, with reproducible outcomes.

RESULTS AND DISCUSSION

PS and SC

The PS and SC of adsorbent nanoflowers (KA1, KA2, KA3, KA4, KA5, and KA6) are stated in Table 2. The PS of the KA6 formulation was measured at 332.96 ± 6.21nm. The nanoflower distribution was observed to be uniform, and the PS of nanoflowers was regulated by keeping the CS and STPP ratio at 1:3.5. To ascertain the surface charge of formulation KA6, the zeta potential of adsorbent nanoflowers was examined which was found to be -14.10±0.16 mV. The nanoflowers' SC plays a key influence in the colloidal stability of the formulation. The results obtained indicate the stability and uniform distribution of particles in nanoflowers. The SC is the main factor responsible for the adsorption of NFs and other factors which influence the NFs are: method of synthesis, pH, PS, and environmental condition. The adsorbent nanoflowers for bilirubin estimation were formulated by the ionotropic gelation technique. In the formation of adsorbent nanoflower KA6, due to complexation with STPP, CS underwent gelation. From the anionic charge of the adsorbent nanoflower, it is possible to extrapolate that polyelectrolyte complexation between the polymer and cross-linker causes anionic STPP to adhere to the surface of the cationic polymer.

FE-SEM

FE-SEM was performed to determine the surface morphology of formulation KA6, and surface morphology showed flower-shaped structures; Figure 1 depicts surface morphology of formulation KA6. The results of FE-SEM indicated the formation of flower-shaped nanoflowers due to the complexation of CS and STPP. The ionotropic gelation technique was used for the preparation of the adsorbent NFs and the diameter of NFs increased with a higher concentration of polymer while the size of NFs reduced with increasing concentration of the cross-linking agent. The SEM results showed the formation of flower-like nanoformulation with closely packed petals and average particle size in the range of 200-500 nm. The nanoflowers possessed a higher surface area, as a result of the large number of closely packed petals encircling the core of the formulation [16].

TEM

The morphological characteristics and structure of nanoflowers were studied using TEM and Figure 2 illustrates the surface morphology of NFs KA6. The surface morphology of formulation KA6 showed a petal-like

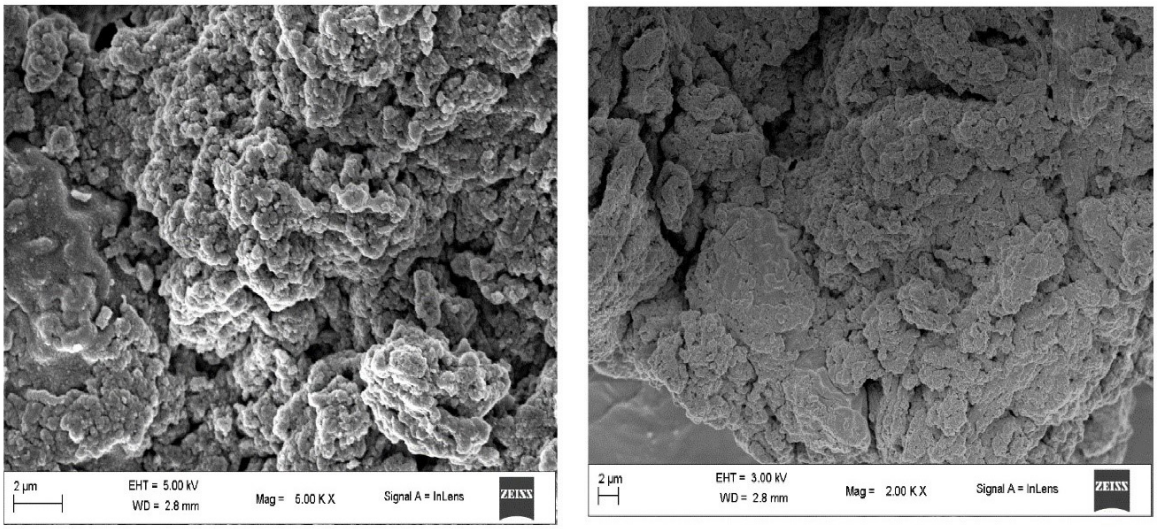

Figure 1. **SEM images of formulation KA6**.

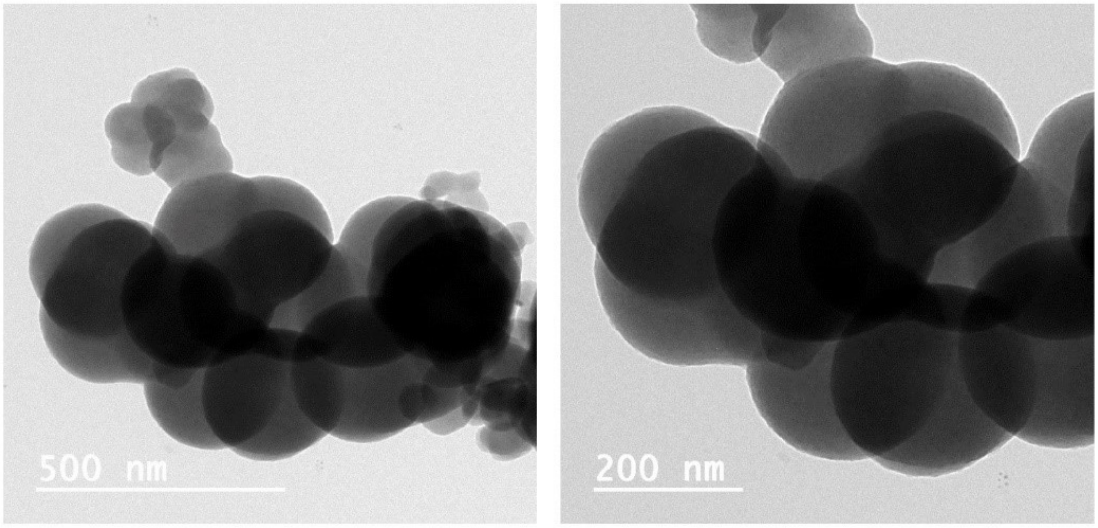

Figure 2. **Transmission electron micrographs of formulation KA6**.

structure and the particle size of the formulation ranging between 200-500 nm. The effective complexation between CS and STPP in adsorbent nanoflowers developed with the inotropic gelation technique was due to the effective complexation between CS and STPP [17].

ATR-FTIR Spectroscopy

The ATR-FTIR study of CS studied at 400-4000 cm^{-1} showed a peak at 1174 cm^{-1} for (C-O-C) and 2865 cm^{-1} attributed to the presence of the CH_2 group. The characteristic peaks of STPP were observed at 1124.7 cm^{-1} and 915.7 cm^{-1} suggesting the presence of (P=O) and (P-O-R). FTIR study of formulation KA6 showed a peak at 1635.07 cm^{-1} assigned to CO-O stretching and 325.54 cm^{-1} attributed to O-H stretching. ATIR-FTR analysis of NFs KA6 showed effective complexation between polymer and cross-linker, CS and STPP, resulting in the formation of NFs. The shift in the peak of O-H bending from 3247 to 3319 cm-1 indicated the electrostatic interaction between CS and STPP with increased interaction of hydrogen bond in CS. In the formation of adsorbent NFs, the peak associated with CS showed a shift from 1589 to 1543 cm-1 indicating the presence of the C=O amide group. Symmetrical stretching of NH_2 and C=O amide group from 750-512 cm^{-1} confirmed interaction amid CS

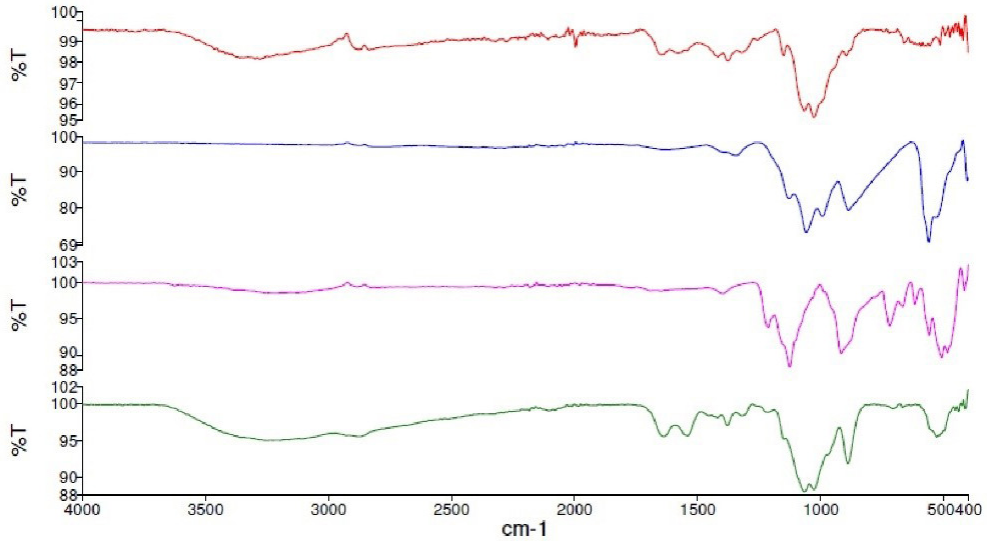

Figure 3. **FTIR-ATR spectra of i) CS, ii) STPP, iii) DCP, and iv) Formulation KA6**.

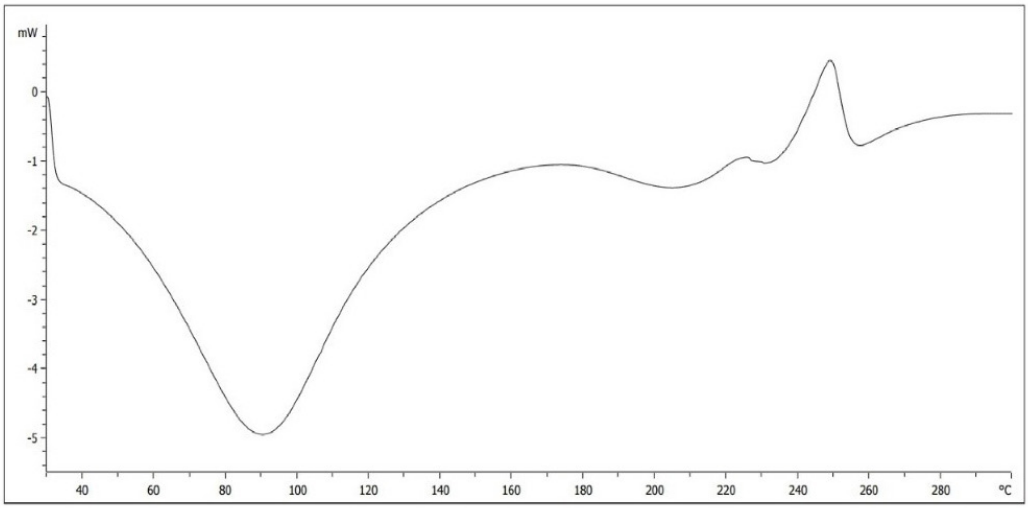

Figure 4. **DSC thermogram of formulation KA6**.

and STPP [18] (Figure 3).

DSC

DSC analysis of formulation KA6 was performed under a temperature range of 30-300ºC and a flow rate of 10ºC/min with a nitrogen purge. The thermogram of nanoflower formulation KA6 (Figure 4) demonstrated the endothermic and exothermic peaks at 90.32°C and 249.02°C, respectively. The water evaporation associated with the CS resulted in the endothermic peak of formulation KA6 at 90.32°C while the exothermic peak of formulation KA6 observed at 249.02°C attributed to the changes in the formulation KA6 due to molecular interaction between polymer and cross-linker, thereby indicating the development of complex between CS and STPP. The shift in the peak of the DSC thermogram for formulation KA6 indicates the complexation between CS and STPP, due to the electrostatic interaction of the polymer with the cross-linker, thereby confirming the development of NFs [19].

TGA and DTA

TGA and DTA analysis of the formulation KA6 depicts the thermal behavior of adsorbent nanoflowers. Thermal analysis (TGA and DTA curve) of formulation carried out within a certain range of temperature between 37ºC to 800ºC is demonstrated in Figure 5a,b. The TGA

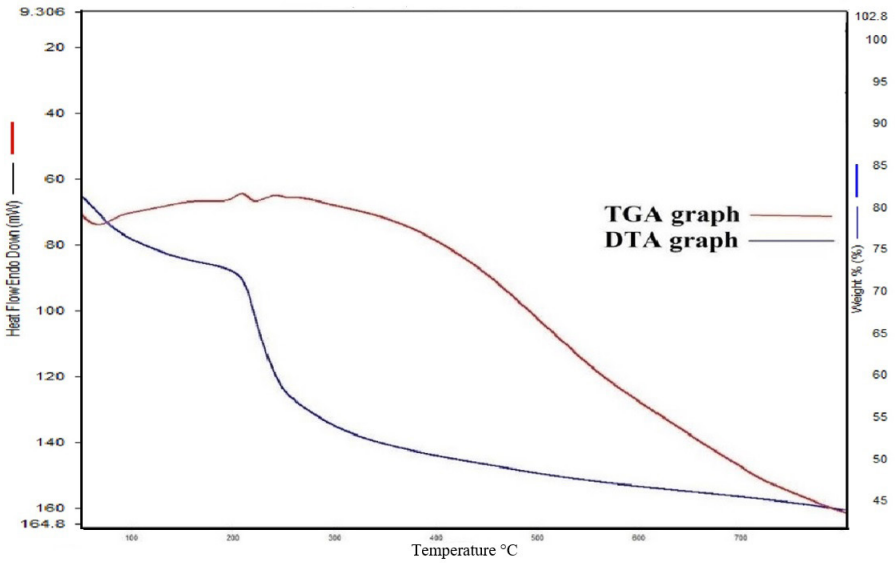

Figure 5. (**a**).**TGA graph of formulation KA6 and** (**b**). **DTA graph of formulation KA6**.

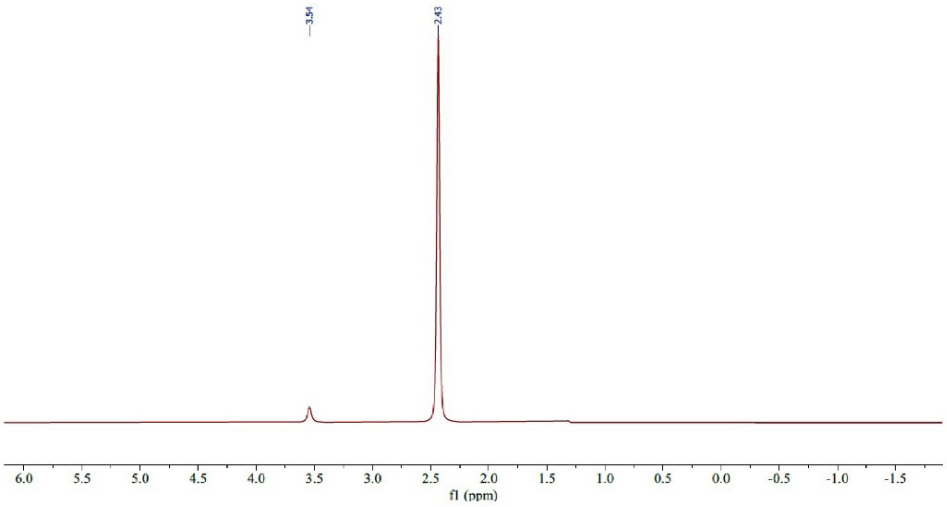

Figure 6. **^{1}H NMR spectrum of formulation**.

graph of formulation showed the loss in weight of mass from 99.09% to 43.01% in the temperature range of 29.16ºC to 806.70ºC. The DTA graph of KA6 analogous to the temperature axis indicated the endothermic peak after 710ºC. Crosslinking of CS with STPP resulted in increased thermal stability of NFs. From the findings of the TGA curve, it was observed that the thermal analysis of formulation did not have signal association thereby, confirmed successful complexation between polymer and cross-linker. The intermolecular interaction between CS and STPP confirmed thermal stability concerning adsorbent NFs [20,21].

^{1}H NMR

The complexation formed in the formulation KA6 between CS and STPP was confirmed by the ^{1}H NMR spectrum. Figure 6 shows the peaks of formulation KA6 in ^{1}H NMR by using DMSO as the solvent at 3.54ppm and 2.43 ppm. The ^{1}HNMR peak shown at 2.43ppm depicts the peak of residual solvent DMSO-d_5, while the peak observed at 3.54ppm is the characteristic peak of proton in CS (-OCH_3). The ^{1}H NMR reported the peak of CH_3 residue and the peak of protons (H2, H3, H4, H5, and H6) in the CS backbone from 2.43 ppm to 3.54 ppm. As reported in the literature and from the result of the intermolecular interaction between CS and STPP, findings from the ^{1}H NMR spectrum of formulation KA6 provided confirmation of the development of adsorbent

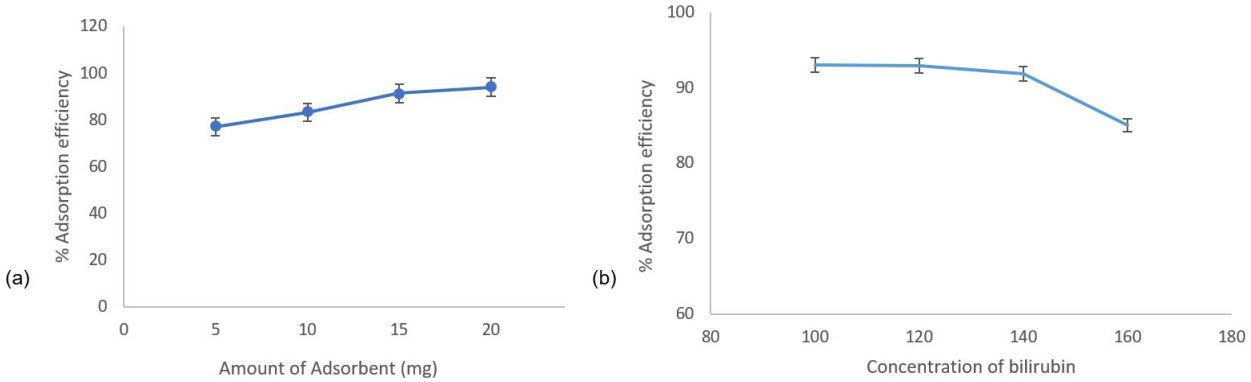

Figure 7 (**a**). **Influence of bilirubin levels on adsorption and** (**b**). **Impact of the quantity of adsorbent on bilirubin adsorption**.

NF [17,22].

In Vitro Adsorption Study of Biosensor-based Nanoflowers

Influence of Bilirubin Levels on Adsorption: The effect of bilirubin concentration on % AE of adsorbent NFs formulation KA6 is shown in Figure 7. The % AE of nanoflowers decreased from 93.05% to 85.03% when the concentration of bilirubin increased from 100 PPM to 160 PPM. The results of bilirubin concentration on nanoflower adsorption revealed that when bilirubin concentration was increased, the adsorption effectiveness of nanoflowers decreased. The lower adsorption sites available for bilirubin adsorption with a higher concentration of bilirubin thereby indicate the reduction in % AE of nanoflowers [23].

Impact of the Quantity of Adsorbent Nanoflowers: The impact of the quantity of nanoflowers (6, 12, 18, 24, and 30 mg) of NFs KA6 on the adsorbent efficiency of bilirubin is depicted in Figure 7b. In formulation KA6, the greatest adsorption effectiveness of nanoflowers for bilirubin determination was reported at 25mg. When the amount of adsorbent was raised from 5mg to 25mg, the % AE of NFs for bilirubin adsorption enhanced from 87.32% to 90.13%. As a result of the impact of the quantity of nanoflowers, the % AE of nanoflowers for bilirubin estimation shows linear growth as the amount of adsorbent is increased. The linearity between % AE and amount of adsorbent was largely by the virtue of, with an increased amount of adsorption, available effective area for adsorption of bilirubin also increases, which in turn leads to higher adsorption sites available for bilirubin adsorption and enhances the % AE and adsorption capacity of nanoflowers.

Desorption Study for Adsorbent Nanoflowers: A desorption study of nanoflowers was performed for the reusability of nanoflowers. From the desorption studies of adsorbent nanoflowers, it was observed that the % AE of nanoflowers reduces after repeated use. The loss of activity in the adsorbent nanoflowers was noticed after the second run. Henceforth, the nanoflowers for bilirubin estimation could be used for two runs after which the % AE reduces [16] (Figure 8).

Comparative Study of Bilirubin Adsorption of Pathology Sample by Nanoflowers and Diagnostic Kit: The comparative study of bilirubin estimation in pathology samples with adsorbent nanoflowers and a diagnostic kit was carried out to evaluate the efficiency of adsorbent NFs (Table 3) In pathology sample analysis with adsorbent NFs, the bilirubin concentration of patients was observed to be 1.2 mg/dL, 0.9 mg/dL, 1.4 mg/dL, 1.0 mg/dL, 0.8 m/dL, patient 1, 2, 3, 4, and 5 respectively. In pathology sample analysis with diagnostic kit, the bilirubin concentration was found to be 1.3 mg/dL, 1.1 mg/dL, 1.3 mg/dL, 1.1 mg/dL, and 0.8 mg/dL, patient 1, 2, 3, 4, and 5, respectively. Similarly with negative urine samples, the bilirubin concentration was found to be 0.02 mg/dL, 0.01 mg/dL, 0.00 mg/dL, 0.01 mg/dL, and 0.00 mg/dL, patient 1, 2, 3, 4 and 5 respectively. From the results of the pathology sample study, it was observed that the normal range of bilirubin concentration was within the limits of 0.1-0.9 mg/dL. The pathology sample study indicated a higher concentration of bilirubin in patients. The results from the comparative study of pathology sample with adsorbent nanoflowers and diagnostic kit [24], showed the efficiency of adsorbent nanoflowers for bilirubin estimation in jaundice.

CONCLUSIONS

Adsorbent nanoflowers-based biosensors for bilirubin estimation were prepared by ionotropic gelation technique to enhance the adsorption behavior of bilirubin and accurate and sensitive detection of bilirubin in jaundice. The prepared nanoflower-based biosensor was evaluated for adsorption of bilirubin and comparative study of bilirubin adsorption by nanoflowers from solution and arti-

Table 3. Comparative Study of Bilirubin Adsorption of Pathology Sample

Patient	Adsorbent flowers (mg/dL)	Diagnostic kit (mg/dL)	Negative controls (mg/dL)
1	1.2	1.3	0.02
2	0.9	1.1	0.01
3	1.4	1.3	0.00
4	1.0	1.1	0.01
5	0.8	0.8	0.00

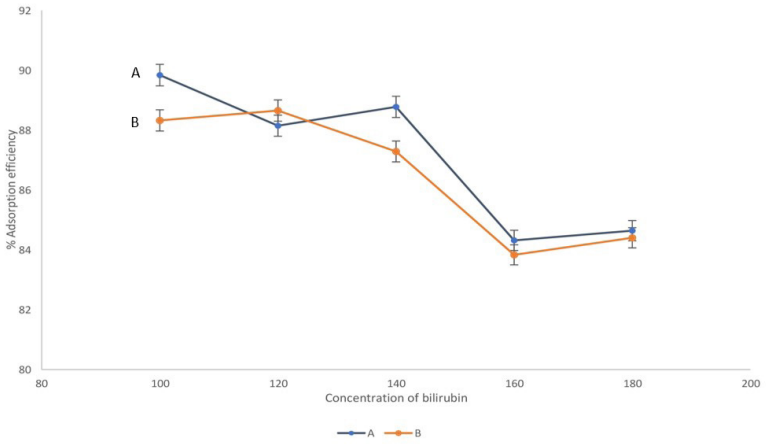

Figure 8. Desorption and after desorption study of adsorbent nanoflowers (A-primary sample and b-repeated use).

ficial urine sample and pathological sample analysis for adsorption of bilirubin. The particle size of nanoflower KA6 was in the range of 300-500 nm with zeta potential (surface charge) in the range of -14.01±0.16 mV to -15.90±0.57 mV. ATIR-FTIR spectroscopy study of formulation KA6 showed effective complexation between polymer and cross-linker thereby indicating the formation of a complex that confirmed the formation of nanoflowers. DSC thermogram of formulation KA6 indicated the development of nanoflowers due to polyelectrolyte complexation of polymer and crosslinker. The % AE of NFs-based biosensors was found to be 90.12%. With increased available surface area, higher adsorption sites, with enhanced adsorption capacity, biosensor-based NFs showed exceptional ability as the nanoparticulate system in bilirubin quantification in jaundice. The prepared biosensor-based nanoflower showed a higher potential for estimation of bilirubin in jaundice, but specificity was not explored in this study.

Conflict of Interest: The authors declare that there are no conflicts of interest.

REFERENCES

1. Shende P, Kasture P, Gaud RS. Nanoflowers: the future trend of nanotechnology for multi-applications. Artif Cells, Nanomedicine Biotechnol. 2018;46(sup1):413–22. https://doi.org/10.1080/21691401.2018.1428812.
2. Perumal V, Hashim U, Gopinath SC, Haarindraprasad R, Foo KL, Balakrishnan SR, et al. "Spotted Nanoflowers": gold-seeded zinc oxide nanohybrid for selective bio-capture. Sci Rep. 2015 Jul;5(1):12231.
3. Wu ZF, Wang Z, Zhang Y, Ma YL, He CY, Li H, et al. Amino acids-incorporated nanoflowers with an intrinsic peroxidase-like activity. Sci Rep. 2015 Jun;2016(6):1–7.
4. Wang X, Shi J, Li Z, Zhang S, Wu H, Jiang Z, et al. Facile one-pot preparation of chitosan/calcium pyrophosphate hybrid microflowers. ACS Appl Mater Interfaces. 2014 Aug;6(16):14522–32.
5. Zhang G, Deng C, Shi H, Zou B, Li Y, Liu T, et al. ZnO/Ag composite nanoflowers as substrates for surface-enhanced Raman scattering. Appl Surf Sci. 2017;402:154–60.
6. Shende P, Kasture P. Bioconjugated nanoflower for estimation of glucose from saliva using nanozymes. Mater Technol. 2022;37(8):842–8.
7. Khan RS, Houlihan DD, Newsome PN. Investigation of jaundice. Med (United Kingdom). 2019;1–5. https://doi.org/10.1016/j.mpmed.2019.08.011.
8. Khan I, Saeed K, Khan I. Nanoparticles: Properties, applications and toxicities. Arab J Chem. 2019;12(7):908–31.
9. Wang X, Chowdhury JR, Chowdhury NR. Bilirubin metabolism: applied physiology. Curr Paediatr. 2006;16(1):70–4.
10. Roy-Chowdhury N, Wang X, Roy-Chowdhury J. Bile pigment metabolism and its disorders. Seventh Ed. Emery and Rimoin's Principles and Practice of Medical Genetics

and Genomics: Cardiovascular, Respiratory, and Gastrointestinal Disorders. Elsevier; 2019. 507–553 p.
11. Ngashangva L, Bachu V, Goswami P. Development of new methods for determination of bilirubin. J Pharm Biomed Anal. 2019 Jan;162:272–85.
12. Rawal R, Kharangarh PR, Dawra S, Tomar M, Gupta V, Pundir CS. A comprehensive review of bilirubin determination methods with special emphasis on biosensors. Process Biochem. 2020;89:165–74.
13. Bergmeyer HU, Horder H, Rej R. Approved Recommendation (1985) on IFCC Methods for the Measurement of Catalytic Concentration of Enzymes. IFCC Method for Alanine Aminotransferase. J Clin Chem Clin Biochem. 1986;24(7):481–95.
14. Kurosaka K, Senba S, Tsubota H, Kondo H. A new enzymatic assay for selectively measuring conjugated bilirubin concentration in serum with use of bilirubin oxidase. Clin Chim Acta. 1998 Jan;269(2):125–36.
15. Zelenka J, Lenícek M, Muchová L, Jirsa M, Kudla M, Balaž P, et al. Highly sensitive method for quantitative determination of bilirubin in biological fluids and tissues. J Chromatogr B Analyt Technol Biomed Life Sci. 2008 May;867(1):37–42.
16. Giri TK, Thakur A, Alexander A, Ajazuddin, Badwaik H, Tripathi DK. Ajazuddin, Badwaik H, Tripathi DK. Modified chitosan hydrogels as drug delivery and tissue engineering systems: present status and applications. Acta Pharm Sin B. 2012;2(5):439–49.
17. Shende P, Sahu P, Gaud R. A technology roadmap of smart biosensors from conventional glucose monitoring systems. Ther Deliv. 2017 Jun;8(6):411–23.
18. Devlekar NP, Shende P. Green synthesis of adsorbent nanoflowers for efficient removal of toxins. Chem Zvesti. 2022;76(4):2209–19.
19. Zhao L, Duan X, Cao W, Ren X, Ren G, Liu P, et al. Effects of different drying methods on the characterization, dissolution rate and antioxidant activity of ursolic acid-loaded chitosan nanoparticles. Foods. 2021 Oct;10(10):2470.
20. Hashad RA, Ishak RA, Fahmy S, Mansour S, Geneidi AS. Chitosan-tripolyphosphate nanoparticles: optimization of formulation parameters for improving process yield at a novel pH using artificial neural networks. Int J Biol Macromol. 2016 May;86:50–8.
21. Lassoued A, Lassoued MS, Dkhil B, Ammar S, Gadri A. Synthesis, structural, morphological, optical and magnetic characterization of iron oxide (α-Fe2O3) nanoparticles by precipitation method: Effect of varying the nature of precursor. Phys E Low-Dimensional Syst Nanostructures. 2018;97(2018):328–34.
22. Gohi BF, Zeng HY, Cao XJ, Zou KM, Diao Y, Diao Y. Preparation of the hybrids of hydrotalcites and chitosan by urea method and their antimicrobial activities. Polymers (Basel). 2019 Sep;11(10):1588.
23. Silvestro I, Francolini I, Di Lisio V, Martinelli A, Pietrelli L, Scotto d'Abusco A, et al. Preparation and characterization of TPP-chitosan crosslinked scaffolds for tissue engineering. Materials (Basel). 2020 Aug;13(16):3577.
24. Kaur K, Rani S, Mahajan K. Congo Red Biowaste Materials as Adsorbents. J Chem. 2012;2013:12.